Food Control 152 (2023) 109831

Contents lists available at ScienceDirect

Food Control

journal homepage: www.elsevier.com/locate/foodcont

Analysis of a quantitative risk assessment of listeriosis from pasteurized milk: The combinations of which factors cause listeriosis in this low-risk food?

Hiroki Abe [a,b,**], Alberto Garre [a], Shige Koseki [b], Heidy M.W. den Besten [a], Marcel H. Zwietering [a,*]

[a] Food Microbiology, Wageningen University & Research, PO Box 17, 6700 AA, Wageningen, the Netherlands
[b] Graduate School of Agricultural Science, Hokkaido University, Kita-9, Nishi-9, Kita-ku, Sapporo, 060-8589, Japan

ARTICLE INFO

Keywords:
Risk Analysis
sensitivity analysis
low-risk products
Listeria monocytogenes
dairy

ABSTRACT

This study proposes a novel methodology for risk assessment of products with extremely low risk. The method is based on the analysis of those iterations that result in illness occurrence. It is demonstrated using a hypothetical scenario on listeriosis from pasteurized milk heated at 72°C–75 °C for 15–20 s and analysed which combinations of factors resulted in illness. Sixty-one cases of listeriosis were predicted from 10 billion simulations, representing a realistically large number of servings for this product. According to the model simulations, the illness cases were caused by extremely high doses resulting from three rare situations occurring concurrently: high initial level, less effective pasteurization (due to high thermotolerance of *L. monocytogenes* contaminants) and extremely high microbial growth during domestic storage (due to poor storage conditions). However, listeriosis was not always observed even if the three situations occurred. Infectivity (dose–response parameter) had the strongest relevance to illness occurrence. Notably, the results of the sensitivity analysis varied depending on the output variable (microbial concentration at exposure or illness occurrence). Furthermore, the correlation-based sensitivity analysis for the illness occurrence provided unreliable results, discouraging this approach for food products with an extremely low illness probability. Considering that number of illnesses and not exposure is the output variable most relevant for risk management, we propose an innovative method based on graphical representations for sensitivity analysis in low-risk products.

1. Introduction

Regardless of how advanced processing and preservation technologies are, the risk of foodborne illnesses will never be completely reduced to zero (Zwietering et al., 2021). A total of 600 million people worldwide annually suffer from foodborne diseases (WHO, 2015). Therefore, to safeguard public health, it is essential to control the risk of foodborne illnesses. The hazard analysis critical control point (HACCP) system has been widely used to manage and control food safety, which is addressed by analysing and controlling biological, chemical, and physical hazards from raw material production and procurement and handling to manufacturing, distribution, and consumption of the finished product. HACCP identifies critical control points (CCPs) from an analysis of the risks during food production and manages the safety of foods by controlling those CCPs. To ensure food safety using this method, it is necessary to identify key factors or combinations of factors that contribute to food safety risks. Despite this, it is difficult to trace back and identify the characteristics of the processes, distribution, and storage until the foods that cause foodborne disease outbreaks are consumed.

In this study, we performed a quantitative microbiological risk assessment (QMRA), to quantify the risk of foodborne illnesses associated with the consumption of pasteurized milk by simulating the effects of environmental conditions and bacterial characteristics on the probability of foodborne illnesses in a model food chain. QMRA combines existing laboratory and surveillance databases with computational techniques to yield models that can predict public health outcomes (Dennis et al., 2002). Furthermore, because it is a computer simulation,

* Corresponding author. Food Microbiology, Wageningen University, PO Box 17, 6700 AA, Wageningen, the Netherlands.
** Corresponding author. Food Microbiology, Wageningen University, PO Box 17, 6700 AA, Wageningen, the Netherlands.
E-mail addresses: hiroki.abe.microbio@gmail.com (H. Abe), marcel.zwietering@wur.nl (M.H. Zwietering).

https://doi.org/10.1016/j.foodcont.2023.109831
Received 22 December 2022; Received in revised form 12 April 2023; Accepted 26 April 2023
Available online 27 April 2023

all the factors in the food chain can be saved to analyse in detail the scenarios that cause foodborne illnesses; this makes it different from the analysis of actual foodborne illness incidents, e.g. using epidemiological methods.

To elucidate the factors that determine the risk of foodborne illnesses, it is necessary to consider the output variable of the QMRA. As part of the output of a QMRA, sensitivity analyses often find the correlation between the input variables (logistic parameter of the chain, kinetic parameters of the microorganism …) and a model output. In most cases, sensitivity analyses for QMRA are focused on the (log) microbial concentration (i.e. exposure) or the (log) risk per serving. Due to the equations typically used for the dose-response model, the illness probability is low at low microbial count and is very low at very low log numbers (Buchanan et al., 2000). Therefore, the left tail of the probability distribution for the exposure is practically not relevant for the actual risk, and can introduce artefacts in the sensitivity analysis. Revealing factors that affect the variability in the actual risk requires correlations that directly indicate the occurrence of foodborne illnesses. In addition, the log concentration and log illness probability, which are often calculated using QMRA, are difficult to grasp intuitively and often confuse risk managers or decision makers. Expressing risk as a natural number—such as whether foodborne illnesses occur or not—would make it easier to understand and more realistic.

The mathematical methods needed to obtain these intuitive outputs can be computationally demanding. Foods distributed on the market are generally safe, since their residual risks are very low (Zwietering et al., 2021). However, regardless of how low the probability is, if the food is consumed in large quantities by a large population, the residual risk accumulates with the amount consumed, and the number of cases of foodborne illnesses increases. To illustrate this, although the risk per serving is higher for unpasteurized milk than for pasteurized milk, a report estimated a higher foodborne illness risk (cases/year/million population) for pasteurized milk food than for unpasteurized milk because of the very large difference in consumption frequency (FDA & FSIS, 2003). Therefore, the risk of foodborne illnesses caused by foods consumed in large quantities should be estimated in conjunction with the number of servings. In this case, it is necessary to adjust the number of simulations according to the number of servings for natural-number QMRA outputs. This results in a large computational load and has not been generally applied in published QMRAs.

Accordingly, in this study, we focused on the pasteurized milk food chain in Western countries as a model with a relatively high food consumption frequency and relatively low food safety risk. We aimed to reveal the relevant factors in the food chain that contribute to causing listeriosis; we also sought to identify the CCPs that should be considered as a priority for control. Unlike in many other QMRAs, in the present one, the actual cases of illness were investigated as natural numbers and were correlated with the input factors. The output type for the present QMRA—illness occurrence—indicates whether the iteration of the simulated scenario caused illness and what factors or combinations of factors were actually responsible for the illness case. People are estimated to consume 5 billion servings of milk in Netherlands in 2017 (Van Gelder, 2021), assuming 1 serving as 200 mL), 16 billion in Japan in 2020 (MAFF (2022), assuming 1 serving as 200 mL) and 87 billion in the US (FDA & FSIS, 2003). Therefore, 10 billion QMRA iterations were conducted in this study. In addition, sensitivity analyses were used to identify the most relevant factors from the food chain both for the illness occurrence and for exposure to the microorganism.

2. Methods

2.1. Thermotolerance model (for Listeria monocytogenes in milk) derived from metadata based on Bayesian inference

2.1.1. Metadata preparation

The thermal resistance of *L. monocytogenes* was described based on data from the scientific literature. We used the dataset of Van Asselt and Zwietering (2006), which includes 226 *D*-values (decimal reduction times in minutes) for 16 strains of *L. monocytogenes* in milk heat treated at temperatures between 50 and 75 °C.

2.1.2. Description and estimation of D-value variability with Bayesian inference

A secondary model for thermotolerance (*D*-values) of *L. monocytogenes* was fitted to the referenced meta-dataset based on Bayesian inference to describe its variation (Log *D* deviation), representing a combination of variability and uncertainty. The Bayesian *D*-value model was constructed based on the most common secondary model for the *D*-value (Equation (1)):

$$\log D \sim \text{Normal}\left(\log D_{ref} - \frac{T - T_{ref,heat}}{z}, \sigma_{\log D}\right) \quad (1)$$

The coefficients $\log D$ and T stand for the *D*-value (min) and the heating temperature (°C) of each referenced dataset. The unknown parameters z and $\log D_{ref}$ represent the *z*-value and the expected *D*-value at the reference temperature ($T_{ref,heat}$). The observed log *D* deviates with respect to this value according to a normal distribution with variance ${\sigma_{\log D}}^2$. For the standard deviation, $\sigma_{\log D}$,the half-Cauchy distribution (location parameter: 0; scale parameter:1) was used as the prior distribution. The half-Cauchy distribution has been recommended and is commonly used for the prior distribution of the scale parameters like variances or standard deviations (Gelman, 2006; Polson & Scott, 2012). The reference temperature for the *D*-value model—$T_{ref,heat}$—was set at 62.3 °C, which was the average temperature of the referenced dataset (Peñalver-Soto et al., 2019). The convergence of the fitting algorithm was evaluated by visual inspection of the trace plots of the Markov Chains and by checking that the r-hat values were close to 1.0.

2.2. Growth model for L. monocytogenes in milk based on Bayesian inference

2.2.1. Metadata preparation

The growth model for *L. monocytogenes* was built based on growth data obtained from ComBase (Baranyi & Tamplin, 2004). The search terms were Organism = Listeria monocytogenes/inocua; Food category: milk; Temperature: 0-20 °C. This search resulted in 111 growth rates for *L. monocytogenes* in milk that were downloaded manually using the functions included in ComBase.

2.2.2. Description and estimation of specific growth rate variation with Bayesian inference

A secondary model for the specific growth rate (μ-values, in log CFU/h) of *L. monocytogenes* in milk was fitted to the referenced meta-dataset using Bayesian inference to describe the variation in specific growth rate, which was a mixture of variability and uncertainty. The Bayesian specific growth rate model was constructed based on a linear relationship (Equation (2)) between $\sqrt{\mu}$ (with μ in $\log_{10}$/h) and the storage temperature (Zwietering et al., 1993).

$$\sqrt{\mu} \sim Normal\left(\sqrt{\mu_{ref} \cdot \frac{T - T_{min}}{T_{ref,growth} - T_{min}}}, \sigma_{\sqrt{\mu}}\right) \quad (2)$$

The $\sqrt{\mu}$ and T were the data reported on each study T_{min} , $\sqrt{\mu_{ref}}$, $T_{ref,growth}$ and $\sigma_{\sqrt{\mu}}$ are unknown parameters (the minimum temperature for growth, the square root of the specific growth rate at the reference temperature for growth and the variance of the error term), estimated with Bayesian inference. For parameter estimation, T_{min} and $\sqrt{\mu_{ref}}$ were assigned uninformative prior distributions—Uniform[-infinite, infinite]. For the estimated standard deviation of $\sqrt{\mu}$, $\sigma_{\sqrt{\mu}}$, the half-Cauchy distribution was used. The reference temperature for the growth rate model, $T_{ref,growth}$, was set at 8.52 °C, which was the average temperature

of the referenced dataset.

2.3. Food chain simulation conditions

This study adopted a simple one-way model (no cross contamination) for simulating the food chains and pathogen growth using Monte Carlo simulation. The exposure assessment model was built as a Modular Process Risk Model (Nauta 2008) with five different modules: storage on farms (growth), pasteurization (inactivation), distribution from factories to retail stores (growth), storage in retail stores (growth), and storage in domestic refrigerators (growth). Microbial inactivation was described using the log-linear primary model, whereas for microbial growth a bilinear model with exponential and stationary phase was used. The QMRA model was solved by Monte Carlo simulations using the input distributions summarized in Table 1 (described in detail below). For reproducibility of the results, the internal seed of the pseudo-random number generator was set before the simulations. The calculations were conducted with Python 3.7.12 using a MacBook Pro, M1, 2020.

2.3.1. Prevalence and initial concentration

The simulated initial concentrations, $Log\ C_0$, in log CFU/mL were defined based on published data. The prevalence and initial concentration of *L. monocytogenes* in milk was characterized as a cumulative distribution (Table 1) derived from two datasets (Dalzini et al., 2016; Meyer-Broseta et al., 2003).

For each iteration, the source of the data is chosen among the two studies with a 50% probability, defining the distribution of both the prevalence and the initial concentration. The presence of *L. monocytogenes* in the milk is defined by the binary variable (0 or 1), W_{cont}, generated by the Bernoulli distribution. If the W_{cont} was 1, the initial concentration was generated using the cumulative distribution derived from the relevant article (Table 1). If the W_{cont} value was 0, all contamination levels in subsequent steps were defined as 0 CFU.

2.3.2. Logistic parameters (time and temperature) for on-farm storage

The distributions of on-farm storage temperature, T_{farm}, (Servello et al., 2004), on-farm storage time, $time_{farm}$, (Barker & Goméz-Tomé, 2013), were used. The on-farm storage temperatures were randomly determined from the cumulative distribution described by Servello et al. (2004) based on data from Canada, and the on-farm times were randomly determined from the PERT distribution referenced by Barker et al. (2013) based on data from the UK (Table 1). The generated storage conditions in this study were assumed to be isothermal during storage and were used for assessing the growth of *L. monocytogenes* in farm storage.

The on-farm storage growth rates were randomly selected from the Bayesian model developed in this study (see above the section: 2.2.). For each iteration, a sample of the posterior distribution of the growth model was taken randomly directly from the Markov chain, obtaining values for the parameters of the secondary growth model (Equation (2)) and the variance value ($\sigma_{\sqrt{\mu},d}$). Then this parameter vector was used in every module involving growth (on-farm, distribution, retail and domestic storage).

After determining the parameter set for the growth behaviour, the root growth rate at the on-farm temperature $\sqrt{\mu_{farm}}$ was determined by a normal distribution using the secondary model (Equation (2)) and the chosen set parameter. To analyse the variability in the specific growth rate, μ, of *L. monocytogenes*, the deviations in $\sqrt{\mu_T}$ were defined as the difference from the median of the preliminary generated 10 thousands simulations of $\sqrt{\mu_T}$. The deviation from median can be the indicator for the variability in growth fitness. Therefore, the deviations were calculated for each temperature.

The Bi-linear model with exponential and stationary phase of the maximum defined as *MPD* (maximum population density) were used for growth estimation during all storage periods in this study. The maximum population density ($\log_{10}$ CFU/mL), *MPD*, was defined as $\mathrm{Uniform}(7.5, 8.5)$ (FDA & FSIS, 2003). The pathogen concentrations after on-farm storage, $Log\ C_{farm}$, were defined as Min ($Log\ C_0 + \mu_{farm} time_{farm}$, *MPD*), according to the Bi-linear models of bacterial growth. The pathogen count increases due to growth by on-farm storage, $\Delta Log\ C_{farm}$, was defined as the difference in the logarithms of pathogen concentration before and after storage as $Log\ C_{farm} - Log\ C_0$.

2.3.3. Heating conditions for pasteurization and the thermotolerance of *L. monocytogenes* in milk

Four different pasteurization conditions (based on Melini et al., 2017) were considered in the QMRA model: 72 °C for 15 s, 72.5 °C for 20 s, 74 °C for 20 s, and 75 °C for 20 s. Furthermore, an additional condition with 85 °C for 20 s was used only for scenario analysis, as described below. The thermal condition used for each iteration was randomly determined among the four with the same probability. After determining the target thermal condition, the magnitude of the temperature deviation, $\varepsilon_{T,heat}$ and time deviation, $\varepsilon_{time,heat}$, was determined in each iteration. As the magnitude of the error could vary, four error patterns were prepared for the heating temperature and time, namely, for the error of heating temperature, ±0.05 °C, ±0.25 °C, ±0.5 °C, and ±1.0 °C, and for that of the error in heating time, 1%, 5%, 10%, and 25%, respectively. The errors for temperature and time were randomly selected with the same probability and adopted in the QMRA simulation. The simulated thermal conditions [heating temperature (°C): T_{heat}; heating time (s): $time_{heat}$] were defined using PERT distributions. The mode of the PERT distribution was assumed as the target thermal condition in each iteration, and the minimum and maximum of the PERT distribution were assumed to be the error of the conditions. To analyse the relevance of the errors in the thermal conditions during sensitivity analysis, the deviation from the target heating conditions was defined as the difference in the heating condition from the target heating conditions of each iteration.

The thermotolerance of the pathogen (*D*-value) was randomly selected using the Bayesian predictive model developed in this study. Similarly, for the growth Bayesian model, the Bayesian model for pathogen reduction has numerous parameter-sets for describing the variations in the estimates. In each MC iteration, the vector of parameters for the secondary model (Equation (1)) and the variance ($\sigma^2_{log\ D}$) were chosen randomly from the Markov chain describing the posteriors of the Bayesian inactivation model [Table 1: Discrete uniform (1, 100000)]. After determining the parameter vector, the logarithm of the *D*-value (min), $\log D_{(T_{heat})}$, taking a random draw from a normal distribution according to Equation (1). To analyse the relevance of variability in the thermotolerance of *L. monocytogenes*, the deviations of $\log D_{(T)}$ for sensitivity analysis were defined as the difference from the median of the preliminary simulated 10 thousands of $D_{(T)}$. The deviations were calculated for each temperature. The *D*-value model was used for estimating the pathogen concentrations after pasteurization, $Log\ C_{heat}$, as $Log\ C_{farm} - \frac{time_{heat}}{60 D_{(T_{heat})}}$ with $time_{heat}$ in s and $D_{(T_{heat})}$ in minutes. The changes of the pathogen concentration by pasteurization, $\Delta Log\ C_{heat}$, was defined as the difference in the logarithms of the pathogen concentration before and after pasteurization as $Log\ C_{heat} - Log\ C_{farm}$.

To consider the effect of a discrete milk volume in a package, the pathogen counts per package were defined as a discrete variable. The package size, $Size_{pack}$, was defined as 1000 mL, and the pathogen counts after packing (CFU/pack), N_{heat_pack}, were simulated by a Poisson distribution as Poisson $(Size_{pack} 10^{Log\ C_{heat}})$. The growth model with Poisson distribution based on Bayesian inference describes the variations in the individual bacterial counts from the average value of the bacterial counts (Vose, 2008). For each iteration, if the draw from the Poisson distribution resulted in zero cells, the microbial concentration was set at 0 CFU for every subsequent module in the simulation.

Table 1
Variables used in simulation. [b,c]

Parameters	Units	Notation	Description	Source
Contaminated probability of bulk tank	(−)	$P_{prevalence}$	$P_{prevalence,i}$	
		i	Classification ([1, 2], [0.5, 0.5]) [a]	
		$P_{prevalence,1}$	0.032	Meyer-Broseta et al. (2003)
		$P_{prevalence,2}$	0.022	Dalzini et al. (2016)
Contaminated occurrence	(−)	W_{cont}	$Bernoulli(< P_{prevalence})$ If contaminated $W_{cont} = 1$, if not $W_{cont} = 0$.	
Initial concentration	log CFU/mL	Log C_0	Log $C_{0,i}$	
		Log $C_{0,1}$	Cumulative ([-7.29, −6.72, −6.14, −5.55, −4.97, −4.40, −3.81, −3.21, −2.64, −2.05, −1.48, −0.905, −0.309, 0.260, 0.830], [9.39×10^{-6}, 2.84×10^{-5}, 5.62×10^{-5}, 1.43×10^{-4}, 6.08×10^{-4}, 1.79×10^{-3}, 6.98×10^{-3}, 0.0163, 0.0603, 0.150, 0.415, 0.776, 0.948, 0.974, 1.0])	Meyer-Broseta et al. (2003)
		Log $C_{0,2}$	Cumulative ([-1.4, 0, 1, 2, 3, 4], [0, 0.128, 0.822, 0.904, 0.941, 1.0])	Dalzini et al. (2016)
Temperature of on-farm storage	°C	T_{farm}	Cumulative ([-0.25, 0.25, 0.75, 1.25, 1.75, 2.25, 2.75, 3.25, 3.75, 4.25, 4.75, 5.25, 5.75, 6.25, 6.75, 7.25, 7.75, 8.25, 8.75, 9.25, 9.75, 10.25, 10.75, 11.25, 11.75, 12.25], [0, 0.000792, 0.000792, 0.00301, 0.0112, 0.06289, 0.151, 0.355, 0.556, 0.723, 0.809, 0.867, 0.910, 0.942, 0.96, 0.983, 0.990, 0.994, 0.997, 0.9987, 0.9992, 0.9996, 0.9998, 0.9998, 0.9998, 1.0])	Servello et al. (2004)
Time of on-farm storage	h	$time_{farm}$	PERT (1.5, 12, 36)	Barker et al., 2013
Growth rate on farm storage	log CFU/mL/h	μ_{farm}	If $T_{farm} < T_{min,d'}$: 0 else: $\left[\text{Normal}\left(\sqrt{\mu_{ref,d'}} \times \frac{T_{farm} - T_{min,d'}}{T_{ref,growth} - T_{min,d'}}, \sigma_{\sqrt{\mu},d'}\right)\right]^2$ $T_{ref,growth}$: 8.52 °C (Mean of dataset) Bayesian MCMC iteration: 100000 Parameters: Mean (S.D.) μ_{ref}: 0.0283 (8.8×10^{-4}) T_{min}: -3.47 (0.54) $\sigma_{\sqrt{\mu}}$: 0.0275 (1.9×10^{-3})	Bayesian model in this study
		d'	Discrete Uniform (1, 100000)	
Maximum population density	log CFU/mL	MPD	Uniform (7.5, 8.5)	FDA, 2003
Concentration after on-farm storage	log CFU/mL	Log C_{farm}	Min (Log $C_0 + \mu_{farm} time_{farm}$, MPD)	Linear growth and stationary model
Temperature of thermal inactivation	°C	T_{heat}	PERT ($T_{heat,k} - \varepsilon_{T,heat,j}, T_{heat,k}, T_{heat,k} + \varepsilon_{T,heat,j}$)	This study
		j	Classification ([1, 2, 3, 4], [0.25, 0.25, 0.25, 0.25]) [a]	
		k	Classification ([1, 2, 3, 4], [0.25, 0.25, 0.25, 0.25]) [a]	
		$T_{heat,1}$	72	Melini et al. (2017)
		$T_{heat,2}$	72.5	This study
		$T_{heat,3}$	74	This study
		$T_{heat,4}$	75	Melini et al. (2017)
		$T_{heat,5}$	85 (Only for scenario analysis)	Melini et al. (2017)
Variation magnitude of heating temperature	°C	$\varepsilon_{T,heat,1}$	0.05	This study
		$\varepsilon_{T,heat,2}$	0.25	
		$\varepsilon_{T,heat,3}$	0.5	
		$\varepsilon_{T,heat,4}$	1	
Time of thermal inactivation	s	$time_{heat}$	PERT ($time_{heat,k}(1 - \varepsilon_{time,heat,l})$, $time_{heat,k}, time_{heat,k}(1 + \varepsilon_{time,heat,l})$)	This study
		l	Classification ([1, 2, 3, 4], [0.25, 0.25, 0.25, 0.25]) [a]	
		$time_{heat,1}$	15	Melini et al. (2017)
		$time_{heat,2}$	20	This study
		$time_{heat,3}$	20	This study
		$time_{heat,4}$	20	Melini et al. (2017)
Variation magnitude of heating time	(−)	$\varepsilon_{time,heat,1}$	0.01	This study
		$\varepsilon_{time,heat,2}$	0.05	
		$\varepsilon_{time,heat,3}$	0.10	
		$\varepsilon_{time,heat,4}$	0.25	
D-value at heating temp.	min	$D_{(T_{heat})}$	$10^{\text{Normal}\left(-\frac{T_{heat} - T_{ref,heat}}{z_{b'}} + \text{Log } D_{ref,b'}, \sigma_{\text{Log } D,b'}\right)}$ $T_{ref,heat}$: 62.3 °C (Mean of dataset) Bayesian MCMC iteration: 100000 Parameters: Mean (S.D.) z: 6.37 (0.14) D_{ref}: 0.81 (0.04) $\sigma_{\text{Log } D}$: 0.29 (0.01)	Bayesian model in this study
		b'	Discrete Uniform (1, 100000)	
Concentration after heating	log CFU/mL	Log C_{heat}	$\text{Log } C_{farm} - \frac{time_{heat}}{60 D_{(T_{heat})}}$	Linear reduction model
Package size	mL	$Size_{pack}$	1000	This study

(*continued on next page*)

Table 1 (*continued*)

Parameters	Units	Notation	Description	Source
Pathogen counts in a package after heating	CFU /pack	N_{heat_pack}	Poisson($Size_{pack}10^{\mathrm{Log}\ C_{heat}}$)	
Temperature of distributing storage	°C	T_{dist}	Normal (6.66, 1.64)	Koutsoumanis et al. (2010)
Time of distributing storage	h	$time_{dist}$	Weibull (1.98, 4.33)	Koutsoumanis et al. (2010)
Growth rate on distributing storage	log CFU/ mL/h	μ_{dist}	If $T_{dist} < T_{min,d'}$: 0 else: $\left[\mathrm{Normal}\left(\sqrt{\mu_{ref,d'}} \times \frac{T_{dist} - T_{min,d'}}{T_{ref.growth} - T_{min,d'}}, \sigma_{\sqrt{\mu},d'}\right)\right]^2$	Bayesian model in this study
Pathogen count after distributing	CFU/ pack	N_{dist}	Min ($N_{heat\_pack} + \mathrm{Negbin}(N_{heat\_pack}, 10^{-\mu_{(T_{dist})}time_{dist}})$; $Size_{pack} \times 10^{\mathrm{MPD}}$)	Linear growth and stationary model
Concentration after distributing	log CFU/mL	Log C_{dist}	$\mathrm{Log}\left(\frac{N_{dist}}{Size_{pack}}\right)$	
Temperature of retail storage	°C	T_{retail}	Normal (4.98, 2.9)	Koutsoumanis et al. (2010)
Time of retail storage	h	$time_{retail}$	Cumulative ([0, 5, 15, 25, 35, 45, 55, 65, 75, 85, 95, 105], [0, 0.0198, 0.443, 0.718, 0.85, 0.916, 0.951, 0.970, 0.982, 0.992, 0.997, 1.0])	Koutsoumanis et al. (2010)
Growth rate on retail storage	log CFU/ mL/h	μ_{retail}	If $T_{retail} < T_{min,d'}$: 0 else: $\left[\mathrm{Normal}\left(\sqrt{\mu_{ref,d'}} \times \frac{T_{retail} - T_{min,d'}}{T_{ref.growth} - T_{min,d'}}, \sigma_{\sqrt{\mu},d'}\right)\right]^2$	Bayesian model in this study
Pathogen count after retail storage	CFU/ pack	N_{retail}	Min ($N_{dist} + \mathrm{Negbin}(N_{dist}, 10^{-\mu_{(T_{retail})}time_{retail}})$; $Size_{pack} \times 10^{\mathrm{MPD}}$)	Linear growth and stationary model
Concentration after retail storage	log CFU/mL	Log C_{retail}	$\mathrm{Log}\left(\frac{N_{retail}}{Size_{pack}}\right)$	
Temperature of domestic storage	°C	$T_{domestic}$	Classification ([Normal (7.57, 2.95), Normal (6.31, 2.66), Normal (6.69, 3.29), Normal (8.40, 3.00)], [0.25, 0.19, 0.05, 0.51]) [a]	Koutsoumanis et al. (2010)
Time of domestic storage	day	$time_{domestic}$	Cumulative ([0, 1, 2, 3, 4, 5], [0, 0.23, 0.74, 0.96, 0.98, 1.0])	Koutsoumanis et al. (2010)
Growth rate on domestic storage	log CFU/ mL/h	$\mu_{domestic}$	If $T_{domestic} < T_{min,d'}$: 0 else: $\left[\mathrm{Normal}\left(\sqrt{\mu_{ref,d'}} \times \frac{T_{domestic} - T_{min,d'}}{T_{ref.growth} - T_{min,d'}}, \sigma_{\sqrt{\mu},d'}\right)\right]^2$	Bayesian model in this study
Pathogen count after domestic storage	CFU/ pack	$N_{domestic}$	Min ($N_{retail} + \mathrm{Negbin}(N_{retail}, 10^{-\mu_{(T_{domestic})}time_{domestic}})$; $Size_{pack} \times 10^{\mathrm{MPD}}$)	Linear growth and stationary model
Concentration after domestic storage	log CFU/mL	Log $C_{domestic}$	$\mathrm{Log}\left(\frac{N_{domestic}}{Size_{pack}}\right)$	
Serving size	mL	$Size_{serve}$	Cumulative ([0, 238, 239, 476, 714], [0, 0.50, 0.75, 0.95, 1.0])	WHO/FAO, 2004
Dose level	CFU	$Dose$	$\mathrm{Poisson}\left(N_{domestic}\frac{Size_{serve}}{Size_{pack}}\right)$	
r-value	(−)	r	Classification ([$r_{Intermediate}$; $r_{Perinatal}$; r_{Elder}], [0.823, 5.71×10^{-3}, 0.171]) [a]	FDA, 2003
		log $r_{Intermediate}$	Normal (−14.11, 1.62)	Pouillot et al. (2015)
		log $r_{Perinatal}$	Normal (−11.70, 1.62)	Pouillot et al. (2015)
		log r_{Elder}	Normal (−12.83, 1.62)	Pouillot et al. (2015)
Illness probability	–	P_{ill}	$W_{cont}(1 - e^{-rDose})$	WHO/FAO, 2004
Illness occurrence	(−)	W_{ill}	$Bernoulli(< P_{ill})$ If illness $W_{ill} = 1$, if not $W_{ill} = 0$	

[a] Classification ([A, B, C], [p_A, p_B, p_C]) denotes the function for divisions to cases; the output value derived from the function is assigned to A with a probability of p_A, to B with a probability of p_B, and to C with a probability of p_C.

[b] The valuables of i, j, k, and l denotes the indicator for divisions to cases.

[c] The b' denotes the indicator for the parameter set number from Bayesian MCMC for the developed reduction model; The d', d'', d''', and d'''' denote the indicators for the parameter set number from Bayesian MCMC for the developed growth model.

2.3.4. Growth of L. monocytogenes during distribution

The growth temperature, T_{dist}, and time, $time_{dist}$, during distribution of the packed milk were randomly determined from published distributions (Koutsoumanis et al., 2010) based on data from Greece which are the normal distributions for T_{dist} and Weibull distribution for $time_{dist}$ (Table 1).

The growth rates during distribution were also randomly determined from the Bayesian model developed in this study in the same manner as the growth rate on the farm. The ID of the parameter set was already determined in the on-farm section, so the root of the growth rate at the distributing temperature $\sqrt{\mu_{dist}}$ was determined by the normal distribution using the secondary model (Equation (2)) and the chosen parameter set. Similar to on-farm growth, the deviations in $\sqrt{\mu_T}$ were calculated for indicating the variability of growth potentials.

The pathogen count per package after growth was calculated as a discrete variable. Therefore, the pathogen count per package after distribution, N_{dist}, was defined as

$$N_{dist} \sim Min\left[N_{heat\_pack} + Negbin\left(N_{heat\_pack}, 10^{-\mu(T_{dist})^{time_{dist}}}\right), \left(Size_{pack} \times 10^{MPD}\right)\right] \quad (3)$$

using the negative binomial distribution describing the stochastic variability in growth with a Bayesian model. The negative binomial distribution is needed in case levels are very low and provides the stochastic prediction as a discrete number based on continuous pathogen concentrations (Vose, 2008). There cannot be 1.4 bacteria in a pack but only either 0, 1, 2 or more. Therefore, the pathogen concentration after distribution, C_{dist}, was derived as $\left(\frac{N_{dist}}{Size_{pack}}\right)$. The increase of pathogen concentration (not log) during distribution, ΔC_{dist}, was defined as the difference in the pathogen concentration before and after distribution as $C_{dist} - \frac{N_{heat\_pack}}{Size_{pack}}$ only if the N_{heat_pack} was not zero. If N_{heat_pack} was zero, the ΔC_{dist} was defined as zero. The following calculation of pathogen concentration changes applies in the same way.

2.3.5. Retail time, temperature, and growth of L. monocytogenes in milk

The distributions of the retail temperature, T_{retail}, and retail storage time, $time_{retail}$, were randomly determined from referenced distributions (Koutsoumanis et al., 2010).

The growth rates and amounts during distribution were also randomly determined from the Bayesian model developed in this study, similar to the growth rate on farms. The pathogen count per package after distribution, N_{retail}, was defined as

$$N_{retail} \sim Min\left[N_{dist} + Negbin\left(N_{dist}, 10^{-\mu(T_{retail})^{time_{retail}}}\right), \left(Size_{pack} \times 10^{MPD}\right)\right] \quad (4)$$

The same as ΔC_{dist}, the increase of pathogen concentration on retail, $\Delta\ C_{retail}$, was defined as $C_{retail} - C_{dist}$.

2.3.6. Growth of L. monocytogenes during domestic storage

The distributions of temperature, $T_{domestic}$, and time, $time_{domestic}$, during domestic storage were randomly determined from the distributions reported by (Koutsoumanis et al., 2010) based on data from Greece. That is, a normal distribution for $T_{domestic}$ and a cumulative distribution for $time_{domestic}$ (Table 1). The description of the increase of pathogen concentration on domestic storage, $C_{domestic}$, was calculated as described above.

2.3.7. Consumption phase and dose-response modelling

The serving size reported by WHO/FAO (2004) was used for $Size_{serve}$ and generated as random numbers following a cumulative distribution (Table 1). The (discrete) dose of *L. monocytogenes* consumed was calculated as a random draw from a Poisson distribution as $Poisson\left(N_{domestic}\frac{Size_{serve}}{Size_{pack}}\right)$. People consuming the simulated milk servings were randomly selected from three types of host populations: intermediate, perinatal, and elderly. The host classification probability was derived based on the reported data of the estimated number of annual servings of pasteurized milk (totally 8.75×10^{10} (FDA & FSIS, 2003)) consumed by these three population groups (intermediate: 7.2×10^{10}, perinatal: 5.0×10^{8}, and elderly: 1.5×10^{10} (FDA & FSIS, 2003)). The illness probability per serving was calculated using an exponential dose-response model ($P_{ill} = 1 - e^{-rDose}$). The r-value of the dose response model was randomly selected for each host population [intermediate: $Normal(-14.11, 1.62)$ perinatal: $Normal(-11.70, 1.62)$, and elderly: $Normal(-12.83, 1.62)$] (Pouillot et al., 2015).

Finally, the illness occurrence, W_{ill}, was calculated from the Bernoulli distribution using the value of P_{ill} calculated from the dose-response model. A value of 1 for W_{ill} indicates the serving-caused illness, whereas a value of 0 indicates that the serving does not cause illness. The number of illness cases was derived from a large number of iterations of the food chain simulation required because of the low risk per serving.

2.4. Sensitivity analysis for identifying the most relevant factors for the risk of listeriosis

Spearman's rank correlation coefficients for the variable factors were derived to elucidate the relevance of each factor to the QMRA results. For comparison, both the correlations of factors against the pathogen log concentration at consumption, $Log\ C_{domestic}$, and against illness occurrence, W_{ill}, were determined. The calculation of Spearman's correlation of 10 billion simulations was conducted and illustrated in the tornado chart for relevance.

2.5. Scenario analysis for different thermal condition targets

To compare the impact of the different heat regimes (72°C–75 °C; 15–20 s, 85 °C; 20 s), the 1 billion iterations of the QMRA model were performed for each heating condition, while the other variables were modified randomly as described above. As the output, not only the illness occurrence, W_{ill}, but also the average of the illness probability per serving, P_{ill}, were derived in the scenario analysis.

3. Results

3.1. QMRA simulation for 10 billion servings for final concentration and illness occurrence

3.1.1. Changes in pathogen concentration in the food chain

Bayesian secondary models describing the inactivation and growth of *L. monocytogenes* in milk at low temperatures were successfully fitted to each metadata set. The estimated 95% credible interval and prediction bands for the secondary models are shown in Fig. S1 (and estimated parameters are used in Table 1).

The changes in *L. monocytogenes* concentrations in the simulated food chains (Fig. 1A) and a boxplot of the initial contamination level (log CFU/mL) and the changing ratio ($\Delta Log\ C$: log CFU/mL; Fig. 1B) are shown, respectively. Ninety nine percent of the initial contamination levels varied from −7.3 to 4.0 log CFU/mL. The changes of the pathogen concentration by pasteurization of whole scenarios had the greatest variance in the changes of concentrations; the median was −20 log CFU/mL, but the 99.99% range was from −474 log CFU/mL to −0.87 log CFU/mL. Furthermore, the variation of the microbial concentration in those cases where illness occurred are illustrated in Fig. 1A as a solid orange line. Each of the 61 orange lines represent the microbial concentration in a scenario that resulted in illness. Compared with the overall changes among all scenarios, the concentration changes of the illness scenarios are extremely rare combinations of three worst-case situations taking place at the same time: high initial contamination level, low reduction in the pasteurization section and large growth during domestic storage. The details of the conditions and concentration changes are listed in Table S1.

The distribution and the place of the illness scenarios of the initial contamination level, growth ratio on farms, reduction ratio by pasteurization, growth ratio on distribution, growth ratio on retail storage, and growth ratio on domestic storage are shown in Fig. 2. The orange bars indicate the location of the specific variable in the particular simulations that resulted in illness. This type of figure, which we designated "barcode chart," makes it easier to compare and understand the specifics of illness scenarios. If the factor does not influence the risk of illness, the orange bars would be distributed evenly according to the sampling distribution in blue (Fig. S2). Otherwise, any clustering of bars in a given area highlights a relationship between the factor represented and the microbiological risk. For example, the survival ratio by pasteurization (Fig. 2C) and the growth during storage (especially domestic, Fig. 2F) seem to be relevant to the illness occurrence, because all illness scenarios in the reductions were higher than the mode of whole distribution (almost −9 log CFU/mL, and many of the illness scenarios in domestic storage were in the extreme upper tail end of the growth

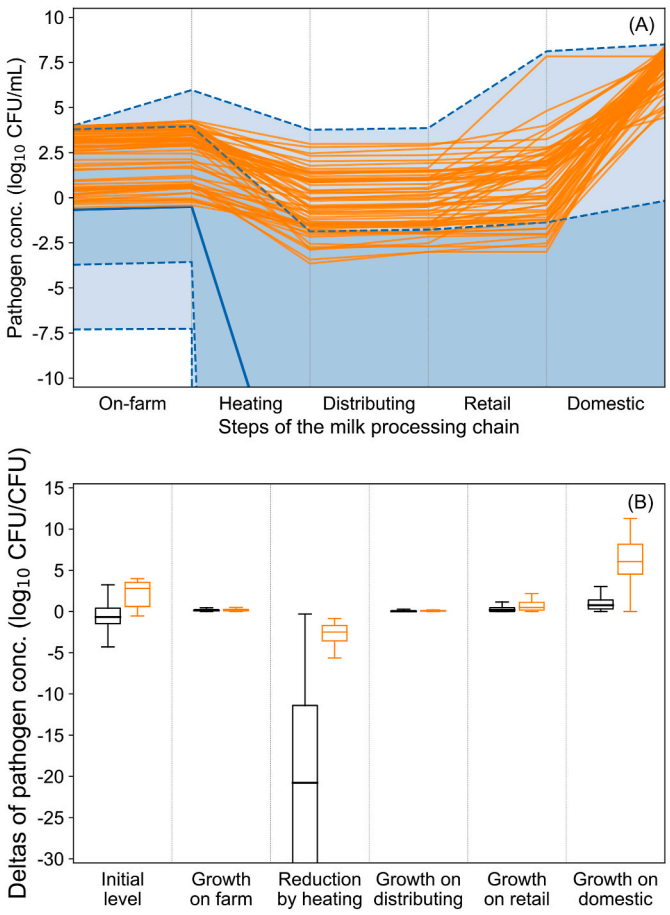

Fig. 1. The comparison of *Listeria* concentration changes for all scenarios and illness occurring scenarios. The prediction band (Panel A; Max-Min: light blue; 99%: blue; median: solid blue line) of the change in *Listeria* concentration in milk during the simulated food chains, and the concentration change in case of illness occurrence (Panel A; 61 orange lines; spaghetti plot). The boxplot of the initial contamination level (log CFU/mL) and the concentration change (log CFU/CFU) by storages and pasteurization in whole scenario (Panel B; black boxplot) and illness occurred scenario (Panel B; orange boxplot). The prediction range and the box plots were based on only the situation of contaminated milk packages.

distribution).

3.1.2. Estimated dose and illness probability of L. monocytogenes per serving of pasteurized milk, and illness cases

In the distribution of the *L. monocytogenes* log dose in the contaminated dose scenario, the zero-dose scenario was omitted because zero CFU would be calculated as minus infinite log CFU. Of all the simulated scenarios, only 0.04% had at least one cell per package of a litre of milk (i.e., 4 in 10,000 packages). Following the same logic as with Fig. 2, Fig. 3 shows a right-hand shift of the orange barcode compared with the blue distribution. The shifts in the pathogen dose indicated that there is a specificity in the dose with listeriosis. The finally contaminated scenario's quantile (0.25, 0.50, and 0.75) was 0.67 log CFU; 1.5 log CFU; 2.5 log CFU. Most simulated dose levels were lower than 6 log CFU, but most of the illness doses were higher than 8 log CFU, and the minimum dose in the illness scenarios was 7.1 log CFU, which is in the extreme upper tail end. The 7.1 log CFU dose was the 1.49×10^{-4} percentile of 10 billion servings. Comparing the doses of the specific illness scenarios with the whole distribution (Fig. 3), the result emphasised that the illness scenarios were all on the extreme tail end of the probability distribution, indicating that the situation in which foodborne illness occurs is an "extreme" outcome (Zwietering, Garre, & Den Besten, 2021; Zwietering, Garre, Wiedmann, & Buchanan, 2021). Moreover, the number of scenarios with higher dose than 7.1 log CFU was 14900. Therefore, the illness cases per all scenarios higher than 7.1 log CFU was 0.4% (61/14900 = 0.0041). This result suggests that even at doses higher than 7.1 log CFU, the illness occurrence is rare.

In a QMRA simulation, 61 cases of illness occurrences were estimated for 10 billion scenarios. Therefore, the illness probability derived from the illness occurrence was 6.1×10^{-9} (risk per serving). This is in accordance with the (arithmetic) average of the illness probability being calculated as 6.16×10^{-9}. Our results from 61 cases of listeriosis per 10 billion servings (6.1×10^{-9}) are similar to those derived from the estimation of QMRAs by other official organizations. The World Health Organization and Food and Agriculture Organization estimated 50 illness cases per 10 billion servings (0.005 cases per 1,000,000 servings) (FAO & WHO, 2004), whereas the Food and Drug Administration estimated 10 illness cases per 10 billion servings (1.0×10^{-9} cases per serving) (FDA & FSIS, 2003). Therefore, our results seem to be at a reasonable order of magnitude.

3.2. Sensitivity analysis of each factor to pathogen log concentration at consumption & illness occurrence

Fig. 4 compares the results of the sensitivity analysis based on Spearman's correlation with respect to the concentration of *L. monocytogenes* at the consumption time (Fig. 4A) and the number of illness occurrence (Fig. 4B). There was a difference in the relative order of the relevance magnitudes. For the final contamination level, the most relevant factor was log *D* deviation ($\rho_{LogD\ deviation|LogC_{domestic}}$: 0.20), followed by heating temperature ($\rho_{T_{heat}|LogC_{domestic}}$: -0.14), initial contamination level ($\rho_{LogC_0|LogC_{domestic}}$: 0.13), and heating time ($\rho_{time_{heat}|LogC_{domestic}}$: -0.12), which had a relatively stronger relevance. The correlations between the storage factors and the variations in the growth rate for the final levels were relatively low ($\rho_{T_{domestic}|LogC_{domestic}}$: 0.00049, $\rho_{time_{domestic}|LogC_{domestic}}$: 0.00048, $\rho_{\sqrt{\mu}_{domestic}|LogC_{domestic}}$: 0.00036, etc.). On the other hand, according to the correlations of illness occurrence, the logarithm *r* parameter of the dose–response model, which indicates variations in the infectivity, had the greatest relevance ($\rho_{Logr|W_{ill}}$: 0.00078), followed by log *D* deviation ($\rho_{LogD\ deviation|W_{ill}}$: 0.00076), domestic storage time ($\rho_{time_{domestic}|W_{ill}}$: 0.00071), domestic storage temperature ($\rho_{T_{domestic}|W_{ill}}$: 0.00068), initial contamination level ($\rho_{LogC_0|W_{ill}}$: 0.00065), heating temperature ($\rho_{T_{heat}|W_{ill}}$: -0.00054), the $\sqrt{\mu}$ deviation on domestic storage ($\rho_{\sqrt{\mu}_{domestic}|W_{ill}}$: 0.00049), and heating time ($\rho_{time_{heat}|W_{ill}}$: -0.00044). Compared to other factors, although the domestic storage conditions had a lower relevance to the final contamination level, the domestic condition was highly relevant to illness occurrence.

The correlation coefficients in Fig. 4B are very small, since theses show the correlation of 61 points having the value 1 (illness occurs) and 10 billion values zero (no illness). The highest correlations found here are indications that the spread of the "ones" is not evenly over the variable of interest and is an indication that a variable is relevant for cases to occur. The correlation coefficients are not significantly different, due to the low number of illness cases in relation to the total number of samples. Both these correlation coefficients and the results from the bar-code chart show the same/similar factors identified as most relevant.

3.2.1. Specifics of the time-temperature condition in illness scenarios

As expected, pasteurization conditions had a high impact on the illness occurrence, with a lower heating temperature and a shorter heating time resulting in more listeriosis cases. There was a left shift of the orange barcode compared to the whole distribution of the heating temperature (Fig. 5A) and a left shift of the barcode compared to the whole distribution of the heating time (Fig. 5B). These results are in line

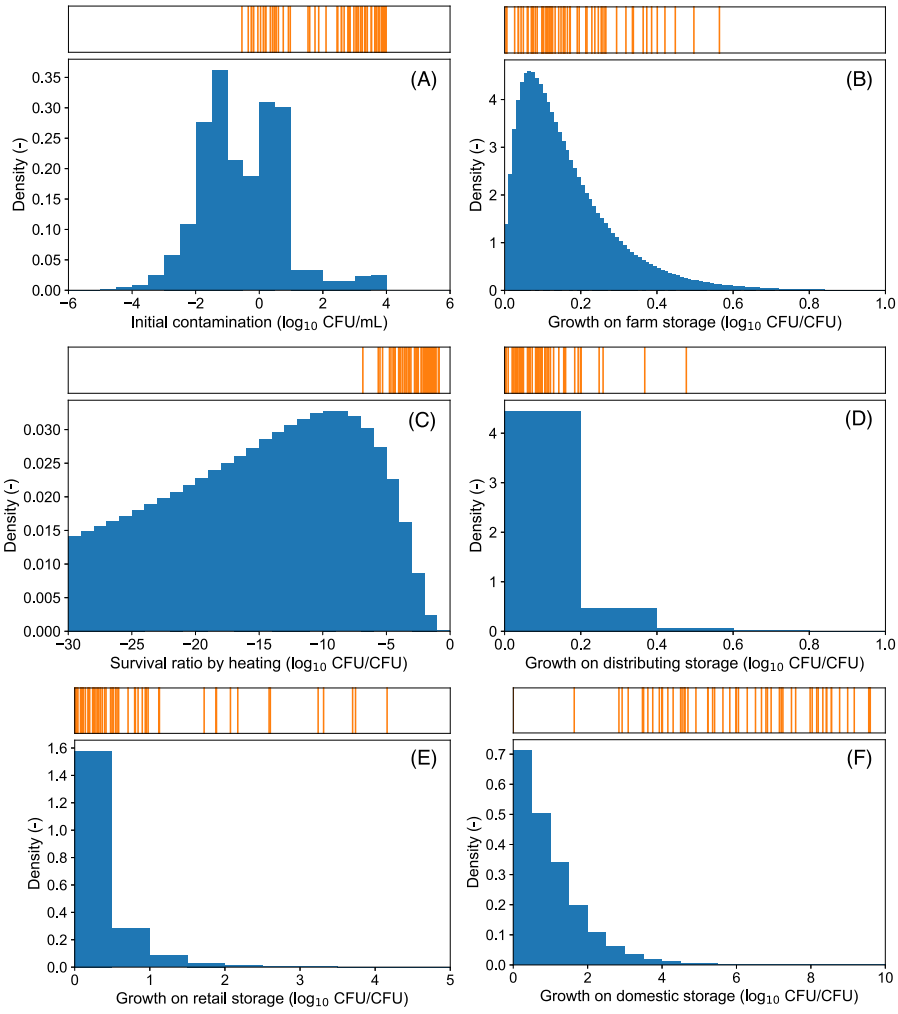

Fig. 2. The frequency distributions of the estimated pathogen behaviour (blue distribution) of *L. monocytogenes* in raw milk and its location in scenarios with illness (orange bars; barcode chart; A: initial contamination level; B: growth ratio on farm storage; C: survival ratio by pasteurization; D: growth ratio on distributing storage; E: growth ratio on retail storage; F: growth ratio on domestic storage). The scale and x-axis grid of the above orange barcode chart is same as that of the below blue distribution. All distributions represent only the contaminated situations in each stage.

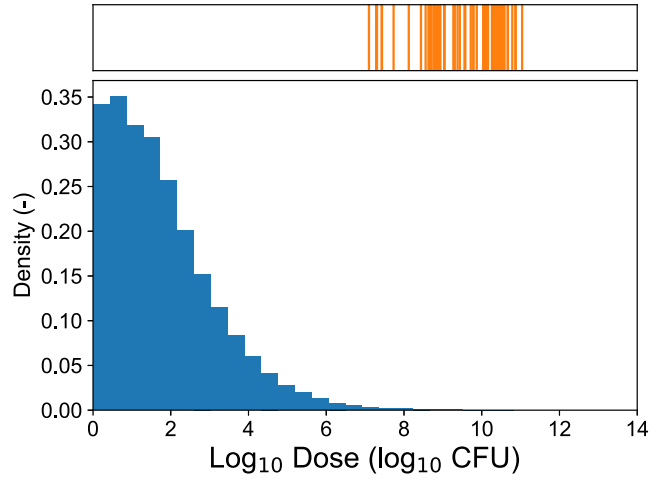

Fig. 3. The distribution of the estimated *L. monocytogenes* dose from contaminated pasteurized milk (blue distribution) and its location in scenarios with illness (orange bar above; barcode chart). The scale and x-axis grid of the above orange barcode chart is same as that of the below blue distribution of Log dose of contaminated dose scenario. The contaminated dose scenario was 0.04% of all scenarios: the doses of the 99.96% of all simulated scenarios were zero.

with the results of the sensitivity analysis based on correlations with respect to the illness occurrence (Fig. 4B). Focusing on the heating target, the 72 °C for 15 s scenario resulted in 47 illness cases; the 72.5 °C for the 20 s scenario resulted in 11 cases; the 74 °C for 20 s scenario resulted in 3 cases; and the 75 °C for 20 s scenario resulted in no illness cases.

For almost all illness scenarios, the pasteurized milk was stored at temperatures higher than 7.5 °C on domestic storage for more than 2 days (Fig. 6). In particular, temperatures higher than 10 °C and durations of more than 4 days had a high density of illness conditions. For the other time–temperature conditions, there was no shift in the barcode chart as compared with the whole distribution (Fig. S2).

3.2.2. *Specifics of pathogen characteristics in the illness scenarios*

The characteristics of the pathogen, which are factors beyond the control of food producers, were also relevant to illness occurrence. There was a clear right shift of the barcode in the thermotolerance deviation of *L. monocytogenes*, the $\sqrt{\mu}$ deviation on domestic storage, and infectivity (Fig. 7) or by adding the times until consumption after pasteurization (Fig. 8). In terms of the other $\sqrt{\mu}$ deviations (on-farm, distributing and retail), there was no shift (Fig. S3). In particular, for thermotolerance and infectivity, all the characteristics for simulations where illness occurred were higher than each mode of the whole distribution (see Fig. 7 and Table S1).

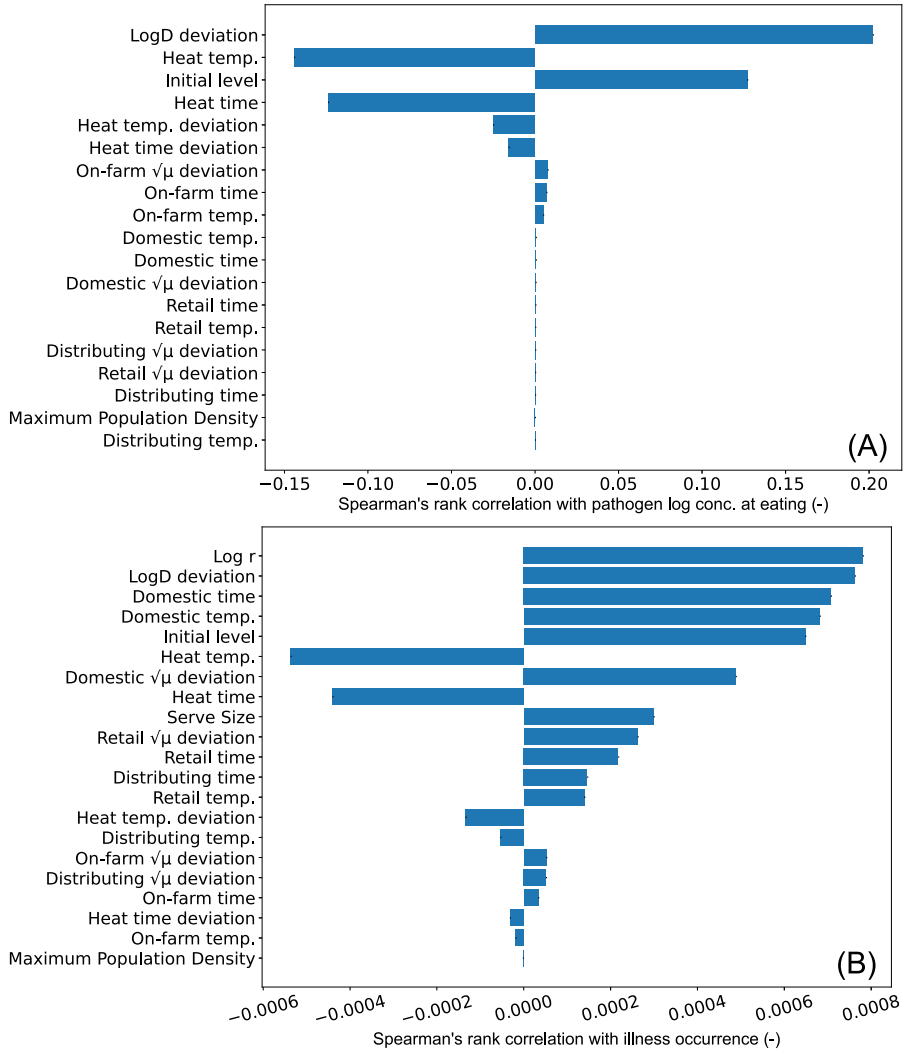

Fig. 4. The Spearman's correlation coefficients of the impact of stochastic variable factors on the final contamination levels of *L. monocytogenes* (in log CFU/ml) at the moment of consumption (A) and on the illness occurrence (B). Factors with stronger correlation coefficients are located at the top.

3.3. Scenario analysis for thermal condition targets

Similar to the results shown in Fig. 5, the scenario analysis for the thermal condition targets indicated that a lower heating temperature and shorter heating time resulted in more cases of listeriosis (Table 2). The average arithmetic risk (the illness probability per serving) in the 72 °C for 15 s scenario was four times that in the 72.5 °C for 20 s scenario, 24.5 times that in the 74 °C for 20 s scenario, and 394 times that in the 75 °C for 20 s scenario. The risk in the 85 °C for 20 s scenario was estimated to be extremely low, lower than the precision of the floating-point arithmetic. Focusing on the occurrences of the cases of listeriosis derived from 1 billion servings, a similar effect of the heating target conditions could be observed although it was difficult to see the differences in extremely low-risk conditions (Table 2). These results were similar to that of illness cases derived from 10 billion QMRA.

4. Discussion

The risk of developing an illness after eating a food in a developed country is extremely small for most products. However, the annual consumption of these products is often in the order of billions, making this small risk per serving still relevant for public health (Zwietering, Garre, Wiedmann, & Buchanan, 2021). Analysing the risk of scenarios with extremely low risk has particular challenges for model definition, calculation and analysis. In this sense, the methodology proposed in this study, which focuses on particular conditions that result in the occurrence of illness, is considered an intuitive, relevant and easy-to-understand analysis method for scenarios with an extremely low risk per serving.

For the development of the methodology, the study used a hypothetical scenario that combines information from different regions. Namely, storage conditions are taken from Greek data, while consumption data represents a survey from the United States of America. Therefore, the risk estimate should not be interpreted as a realistic representation of the situation in either country. Nonetheless, these parameters are in the right order of magnitude for most developed countries, so they clearly exemplify some of the challenges for risk assessment in cases with extremely low risk. As shown by the consumption data from the USA, billions of servings of milk are consumed each year, a result that is also applicable to other developed countries and that makes these products with extremely low risk still relevant for public health. These results are also applicable to other food products with extremely low risk but consumed in great quantities, such as meat.

The methodology developed here is based on the study of those Monte Carlo simulations that resulted in illness occurrence (discrete) and not risk per serving or dose (continuous), provides significant advances in the interpretation of the results of a QMRA model for this type of scenario. In particular, the spaghetti plot (Fig. 1) and the barcode

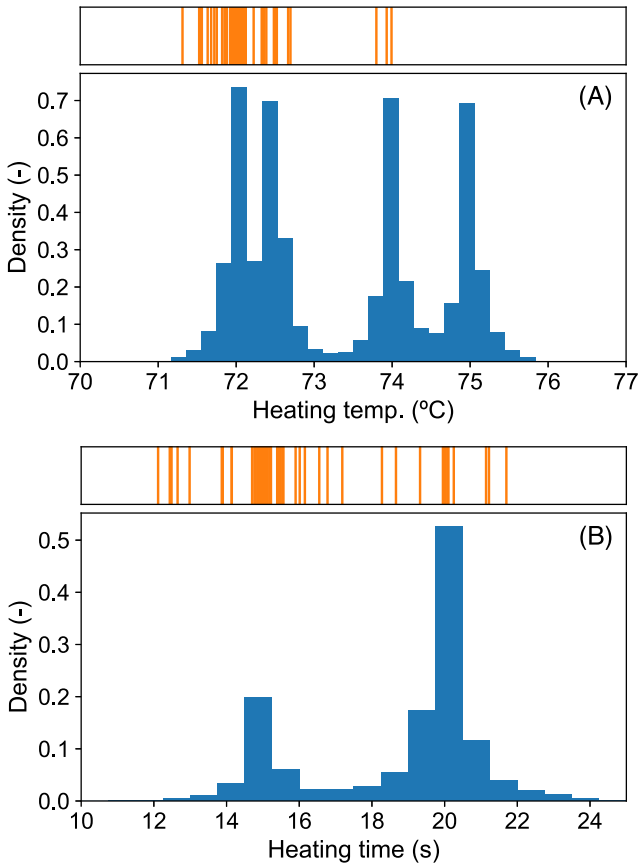

Fig. 5. The distributions of the pasteurization temperature: A and time: B (blue distribution) and its location in scenarios with illness (orange bars). The scale and x-axis grid of the above orange barcode chart is same as that of the below blue distribution.

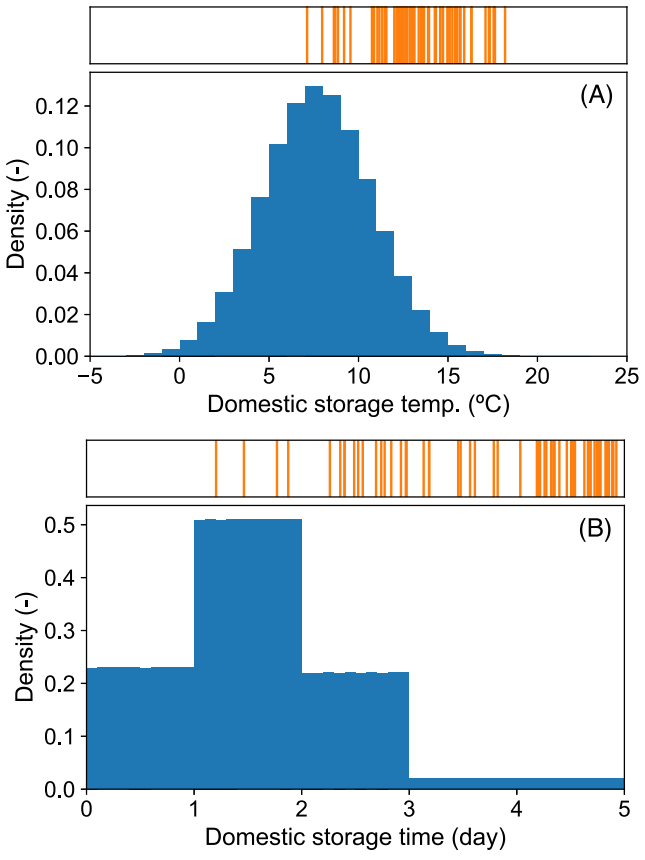

Fig. 6. The distributions of the domestic storage temperature: A and the time: B (blue distribution) and its location in scenarios with illness (orange bars). The scale and x-axis grid of the above orange barcode chart is same as that of the below blue distribution.

charts (Figs. 2, 3, 5 and 6) provide a visual insight on which elements of the food supply chain and which factors are more relevant for the illness occurrence. They show that, for the case studied, illness only takes place when independent, rare events (low reduction in pasteurization, high growth and high pathogenicity) occur at the same time. Therefore, risk managers could control the risk in different ways. One option would be to control heavily one step of the chain (e.g., pasteurization), as illness only occurs if the three steps (reduction, growth and pathogenicity) fail at the same time. A different option would be the application of milder controls on every step independently, as it is very unlikely that every control fails at the same time.

On the other hand, the spaghetti and barcode plot do not provide a clear rank of the model variables, making it hard to prioritize interventions. Hence, it is often advisable to combine this type of analysis with a sensitivity analysis. In this case, we used correlation analysis based on two different output variables: the illness occurrence and the microbial concentration at exposure. We observed that the outcome was strongly dependent on the output variable, due to the sigmoidal behaviour of the dose-response relationship as function of the log dose of *L. monocytogenes*. When the correlation analysis is based on the (log) microbial concentration at exposure, the calculation is based on the whole range of concentrations. However, the dose-response model is practically flat for lower doses. As a result, because the output of the illness occurrence is binary (0 or 1), simulations with low exposure result in the same outcome. This results in a different rank depending on the output variable used for the correlation analysis. Nonetheless, note that these results have been obtained for *L. monocytogenes*, a pathogen with low virulence. It is likely that the dependence on the output variable is not so strong for more virulent pathogens, such as enterohemorrhagic *Escherichia coli*.

Therefore, we emphasize that a risk assessor will need to choose an appropriate target of sensitivity analysis. When consumers' health is the primary concern, focusing on the correlation to the output that directly expresses "whether foodborne illness occurs or not," such as the output style of "illness occurrence" proposed in this study, would be an appropriate method. On the other hand, these correlation coefficients calculated are extremely small, making it hard to make reliable inferences. This is due to the output variable being binary (illness or not) and the very low frequency of illness scenarios (61 cases/10 billions). Therefore, the results of a correlation analysis based on the illness occurrence should be analysed carefully, comparing it to the results of other types of analysis (e.g., barcode plot) and against expert opinion. Furthermore, sensitivity analysis of concentration at the time of consumption can be informative on its own. For instance, since various standards of laws and/or regulations are usually based on the numbers or concentrations of bacteria, the sensitivity analysis to assess final contamination level will be valid for determination of some regulations or performance objectives.

Although the QMRA model has mostly illustrative purposes, there are still some limitations that should be underlined. As mentioned above, the model combines data from different regions. Hence, although there are similarities between them (e.g., both are developed countries), the risk estimates are not a true representation of either region. Furthermore, the model does not include correlations between its variables. For example, storage under temperature abuse often results in obvious spoilage and consumer rejection, reducing the chance of products with high bacterial count being consumed. Therefore, models that

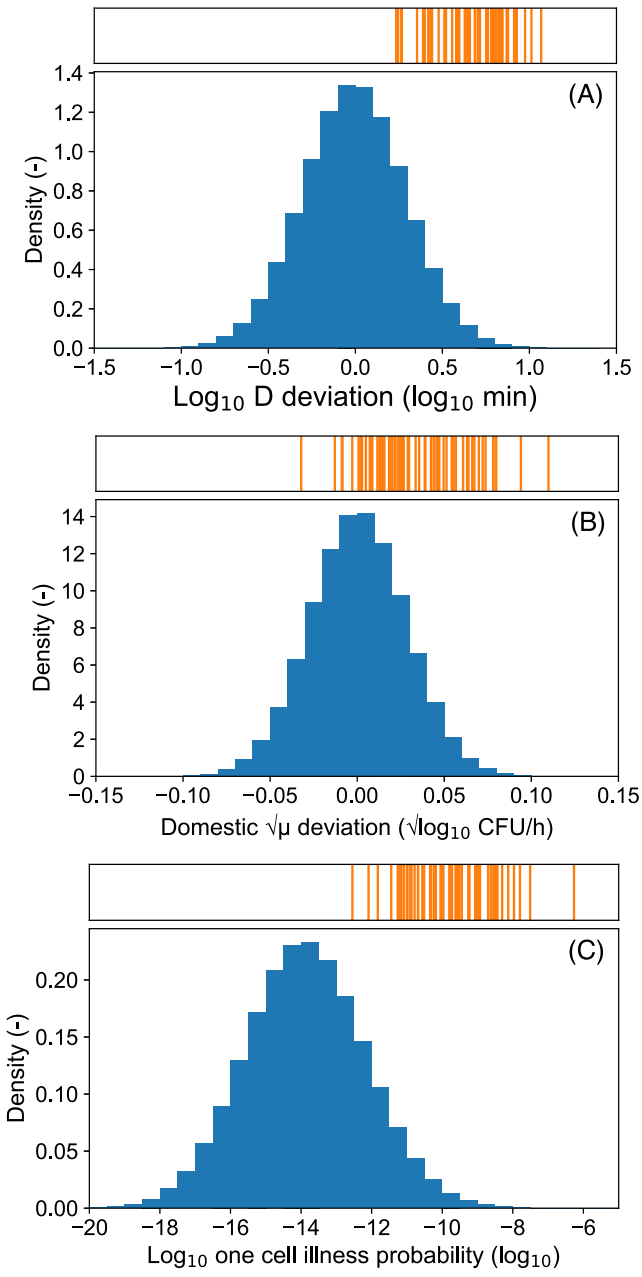

Fig. 7. The distributions (blue) of the Log *D* deviation from the medians at each heating temperature: A, the $\sqrt{\mu}$ deviation during domestic storage: B, the one cell illness probability of dose-response model: C, and its location in scenarios with illness (orange bars). The scale and x-axis grid of the above orange barcode chart is same as that of the below blue distribution.

do not include this kind of correlation tend to overestimate the number of illness cases. Another significant data gap is data on pasteurization conditions (times and temperatures), which is often not publicly available. As illustrated by the results of this study, this uncertainty is highly relevant for the outcome of the risk assessment, as the pasteurization step is critical for the risk estimates.

In conclusion, this article has illustrated some of the challenges related to the assessment of the risk for products with extremely low risk, proposing a novel methodology to address some of them. It focuses on the analysis of the Monte Carlo simulations that result in illness occurrence, either graphically (spaghetti and barcode plots) or by correlation analysis. The method brings valuable insight for risk assessment, being useful to identify which conditions (or combination of conditions) are most likely to result in foodborne illness. Although the method requires a large amount of computation time (409 h per 10 billion simulations on a MacBook Pro, M1, 2020), it is mostly due to the need to simulate billions of Monte Carlo simulations, one per each consumption. Considering the rapid progress in computer performance, it is likely that this problem will lose relevance in the near future.

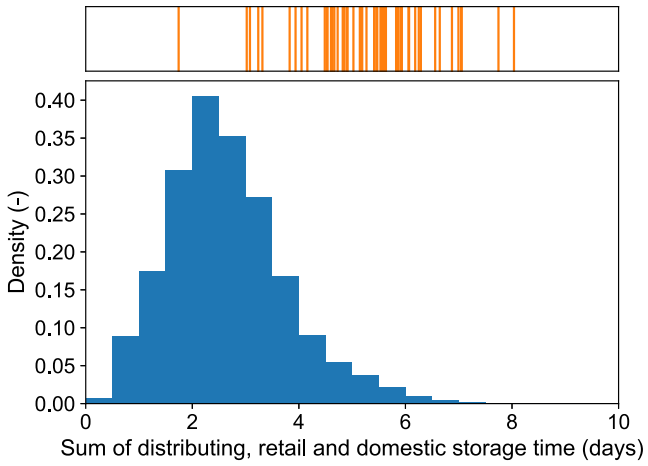

Fig. 8. The distribution (blue) of the post pasteurization time (sum of the storage time of distributing, retail and domestic), and its location in scenarios with illness (orange bars). The scale and x-axis grid of the above orange barcode chart is same as that of the below blue distribution.

Table 2
Results of scenario analysis.

Thermal condition	Average P_{ill}[a]	Illness cases per 1 billion of sensitivity analysis	Illness cases per 1 billion of QMRA MC[b]
72 °C 15 s	2.22×10^{-8}	23	18.8
72.5 °C 20 s	5.48×10^{-9}	6	4.4
74 °C 20 s	9.06×10^{-10}	0	1.2
75 °C 20 s	5.64×10^{-11}	0	0
85 °C 20 s	$<10^{-16}$	0	Not conducted

[a] Average P_{ill} was derived as the average arithmetic risk of simulated scenarios ($\sum_{i=1}^{n} \frac{P_{ill_i}}{n}$; *n*: iteration counts of simulation).
[b] The illness cases of each temperature were divided by 2.5 billion iteration.

Funding Source

The visit of Hiroki Abe has been supported by the JSPS (Japan Society for the Promotion of Science) Overseas Challenge Program for Young Researchers (Recipient number: 202080013).

CRediT authorship contribution statement

Hiroki Abe: Conceptualization, Formal analysis, Software, Writing – original draft. **Alberto Garre:** Conceptualization, Methodology, Software, Writing – review & editing. **Shige Koseki:** Conceptualization, Writing – review & editing. **Heidy M.W. den Besten:** Conceptualization, Methodology, Writing – review & editing. **Marcel H. Zwietering:** Conceptualization, Methodology, Validation, Writing – review & editing.

Declarations of competing interest

The authors declare that they have no known competing financial

interests or personal relationships that could have appeared to influence the work reported in this paper.

Data availability

All the used data and the Python codes are available through co-author GitHub (URL: https://github.com/Hiroki-Abe/Milk_QMRA_of_listeriosis)

Appendix A. Supplementary data

Supplementary data to this article can be found online at https://doi.org/10.1016/j.foodcont.2023.109831.

References

Asselt, E. van, & Zwietering, M. (2006). A systematic approach to determine global thermal inactivation parameters for various food pathogens. *International Journal of Food Microbiology, 107*(1), 73–82. https://doi.org/10.1016/j.ijfoodmicro.2005.08.014

Baranyi, J., & Tamplin, M. L. (2004). ComBase: a common database on microbial responses to food environments. *Journal of Food Protection, 67*, 1967–1971. https://doi.org/10.4315/0362-028X-67.9.1967.

Barker, G. C., & Goméz-Tomé, N. (2013). A risk assessment model for enterotoxigenic *Staphylococcus aureus* in pasteurized milk: A potential route to source-level inference. *Risk Analysis, 33*, 249–269. https://doi.org/10.1111/j.1539-6924.2011.01667.x

Buchanan, R. L., Smith, J. L., & Long, W. (2000). Microbial risk assessment: Dose-response relations and risk characterization. *International Journal of Food Microbiology, 58*(3), 159–172. https://doi.org/10.1016/s0168-1605(00)00270-1

Dalzini, E., Bernini, V., Bertasi, B., Daminelli, P., Losio, M.-N., & Varisco, G. (2016). Survey of prevalence and seasonal variability of *Listeria monocytogenes* in raw cow milk from Northern Italy. *Food Control, 60*, 466–470. https://doi.org/10.1016/j.foodcont.2015.08.019

Dennis, S. B., Buchanan, R. L., & Miller, A. J. (2002). Microbial risk assessment: Achievements and future challenges. https://www.food-safety.com/articles/4444-microbial-risk-assessment-achievements-and-future-challenges.

FAO, WHO. (2004). Risk assessment of Listeria monocytogenes in ready-to-eat foods. *Technical report*. Microbiological risk assessment series no 5. https://www.who.int/publications/i/item/9241562625.

FDA, FSIS. (2003). Quantitative assessment of the relative risk to public health from foodborne Listeria monocytogenes among selected categories of ready-to-eat foods. FDA1–301. https://www.fda.gov/food/cfsan-risk-safety-assessments/quantitative-assessment-relative-risk-public-health-foodborne-listeria-monocytogenes-among-selected.

Gelman, A. (2006). Prior distributions for variance parameters in hierarchical models (comment on article by Browne and Draper). *Bayesian Analysis, 1*(3), 515–534. https://doi.org/10.1214/06-ba117a

Koutsoumanis, K., Pavlis, A., Nychas, G.-J. E., & Xanthiakos, K. (2010). Probabilistic model for *Listeria monocytogenes* growth during distribution, retail storage, and domestic storage of pasteurized milk. *Applied and Environmental Microbiology, 76*(7), 2181–2191. https://doi.org/10.1128/aem.02430-09

Melini, F., Melini, V., Luziatelli, F., & Ruzzi, M. (2017). Raw and heat-treated milk: from public health risks to nutritional quality. *Beverages, 3*, 54–33 https://doi.org/10.3390/beverages3040054.

Meyer-Broseta, S., Diot, A., Bastian, S., Riviere, J., & Cerf, O. (2003). Estimation of low bacterial concentration: *Listeria monocytogenes* in raw milk. *International Journal of Food Microbiology, 80*(1), 1–15. https://doi.org/10.1016/s0168-1605(02)00117-4

Ministry of Agriculture, Forestry and Fisheries (MAFF) of Japan. (2022). Recent situation of milk and dairy product. Retrieved April 21, 2022, from https://www.e-stat.go.jp/stat-search/files/data?sinfid=000032106252&ext=pdf.

Peñalver-Soto, J. L., Garre, A., Esnoz, A., Fernández, P. S., & Egea, J. A. (2019). Guidelines for the design of (optimal) isothermal inactivation experiments. *Food Research International, 126*, Article 108714. https://doi.org/10.1016/j.foodres.2019.108714

Polson, N. G., & Scott, J. G. (2012). On the half-Cauchy prior for a global scale parameter. *Bayesian Analysis, 7*(4), 887–902. https://doi.org/10.1214/12-ba730

Pouillot, R., Hoelzer, K., Chen, Y., & Dennis, S. B. (2015). *Listeria monocytogenes* dose response revisited - incorporating adjustments for variability in strain virulence and host susceptibility. *Risk Analysis, 1–19*. https://doi.org/10.1111/risa.12235

Servello, V., Hill, A. R., & Lencki, R. W. (2004). Towards an optimum mixing protocol for on-farm bulk milk sampling. *Journal of Dairy Science, 87*(9), 2846–2853. https://doi.org/10.3168/jds.s0022-0302(04)73413-x

Van Gelder, K. (2021). Milk consumption in The Netherlands from 2013 to 2019. Retrieved April 21, 2022, from https://www.statista.com/statistics/713835/milk-consumption-in-the-netherlands/#:~:text=Between%202013%20and%202019%2C%20the,to%20roughly%20704%20million%20liters.

Vose, D. (2008). *Risk analysis: A quantitative guide*. Wiley.

WHO. (2015). WHO estimates of the global burden of foodborne diseases: Foodborne diseases burden epidemiology reference group 2007-2015. https://www.who.int/publications/i/item/9789241565165.

Zwietering, M. H., Garre, A., & Den Besten, H. M. W. (2021). Incorporating strain variability in the design of heat treatments: A stochastic approach and a kinetic approach. *Food Research International, 139*, Article 109973. https://doi.org/10.1016/j.foodres.2020.109973

Zwietering, M. H., Garre, A., Wiedmann, M., & Buchanan, R. L. (2021). All food processes have a residual risk, some are small, some very small and some are extremely small: Zero risk does not exist. *Current Opinion in Food Science, 39*, 83–92. https://doi.org/10.1016/j.cofs.2020.12.017

Zwietering, M. H., Wijtzes, T., Rombouts, F. M., & Riet, K. van 't (1993). A decision support system for prediction of microbial spoilage in foods. *Journal of Industrial Microbiology, 12*(3–5), 324–329. https://doi.org/10.1007/BF01584209